This document is the accepted manuscript version of the following article:

Gschwend, D., Müller, S., Wokaun, A., & Vogel, F. (2018). Optimum fuel for spark ignition engines from lignin pyrolysis oil. Energy and Fuels, 32(9), 9388-9398. https://doi.org/10.1021/acs.energyfuels.7b03472

Optimum Fuel for Spark Ignition Engines from Lignin Pyrolysis Oil

Dominik Gschwend,[‡] Sebastian Müller,[‡] Alexander Wokaun,[‡] and Frédéric Vogel[*,‡,¶]

‡*Paul Scherrer Institut (PSI), 5232 Villigen - PSI, Switzerland*

¶*Fachhochschule Nordwestschweiz (FHNW), 5210 Windisch, Switzerland*

E-mail: frederic.vogel@psi.ch

Abstract

Lignin is a high energy content material, which could be used as feedstock for future transportation fuels. To this aim, it needs to be liquefied and upgraded. Currently, the most promising way of upgrading is considered to be hydrodeoxygenation. By combining an upgrading reaction pathway network and a model of a spark ignition internal combustion engine, the fuel properties are linked to the degree of upgrading. This study answers the question how much upgrading is required to obtain the optimum fuel for a spark ignition engine. Depending on the optimization criteria (efficiency, specific CO_2 emissions or volumetric fuel consumption) different selections of compounds are identified both for summer and all year applications. Most of the compounds exhibit a significantly higher efficiency than gasoline at lower volumetric fuel consumption. Specific CO_2 emissions are expected to be marginally reduced compared to gasoline. Furthermore, this study confirms that the initial bio oil is not suitable as fuel and reveals that complete hydrodeoxygenation is not beneficial.

Introduction

Lignin contains roughly 40 % of the energy content of lignocellulosic biomass[1]. However, its chemical recalcitrance hampers its full exploitation. Most of today's biorefinery concepts are missing practicable ways to valorize lignin. Fast pyrolysis is an easy and well-established way to liquefy lignin[2,3]. The different approaches to pyrolysis of biomass have been reviewed and compared[4]. In general, fast pyrolysis leads to three fractions: char, liquid, and gas. The liquid fraction, so called bio-oil, consists of numerous different aromatic and non-aromatic compounds. In general this liquid shows a high acidity, high water content and is chemically instable[5,6]. Therefore the bio-oil is not suited as fuel for Spark Ignition (SI) Internal Combustion Engines (ICEs) and upgrading is indispensable[3,7–9]. To this aim, hydrodeoxygenation (HDO) has been studied to reduce the oxygen content of the compounds and/or to achieve saturation by hydrogen addition[10,11]. Other upgrading strategies and processes have been reviewed and compared to HDO[12]. Several catalysts for the HDO of bio-oil have been tested in long time experiments (up to almost 100 h). Between 33 % to 42 % of the product fell into the gasoline boiling range[13]. Due to the requirement of large quantities of H_2 for HDO the upgrading is expensive[14].

Direct usage of bio-oil as fuel has been studied in Compression Ignition (CI) engines (either marine or converted diesel engines), boilers and gas turbines[15]. While its use in boilers has been demonstrated, the use in engines and turbines is more problematic. Due to the acidic nature of the bio-oil, engines and in particular the fuel systems need to be adapted[16]. In spite of the aromatic nature of the compounds present in the bio-oil, which in general correlated to high Research Octane Numbers (RONs)[17], no reports have been published on experimental studies with SI engines on either raw or upgraded bio oil[18]. In converted diesel engines the low Cetane Number (CN) leads to problems with ignition[16,19]. As CN and RON are inversely correlated, low CN generally result in high RON, indicating potentially good SI fuels. This has been reflected by an experimental study investigating mixtures of upgraded pyrolysis oil, rich in esters, and gasoline[20]. It has been concluded that 10 % of this upgraded

pyrolysis oil in gasoline does not lead to any significant changes over pure gasoline operation. Within this study the question of optimum upgrading has been investigated using a thermodynamic model of an SI ICE in combination with a reaction network.

Lignin derived pyrolysis oil is a mixture of several hundreds of different components. The exact composition depends on the origin of the biomass and on the applied process conditions. In prior studies, the main building blocks (shown in Fig. 1) and the side chains (listed in Figs. 3 to 6) have been identified[10,21,22]. The number of identified substances varies between different studies. Although the occurrence of up to 400 different compounds has been reported[23], the number of exactly identified molecules is in the range of 50. Therefore the number of studied side chains is increased by extrapolation based on the functional groups present in the literature. All possible combinations of main building blocks and side chains

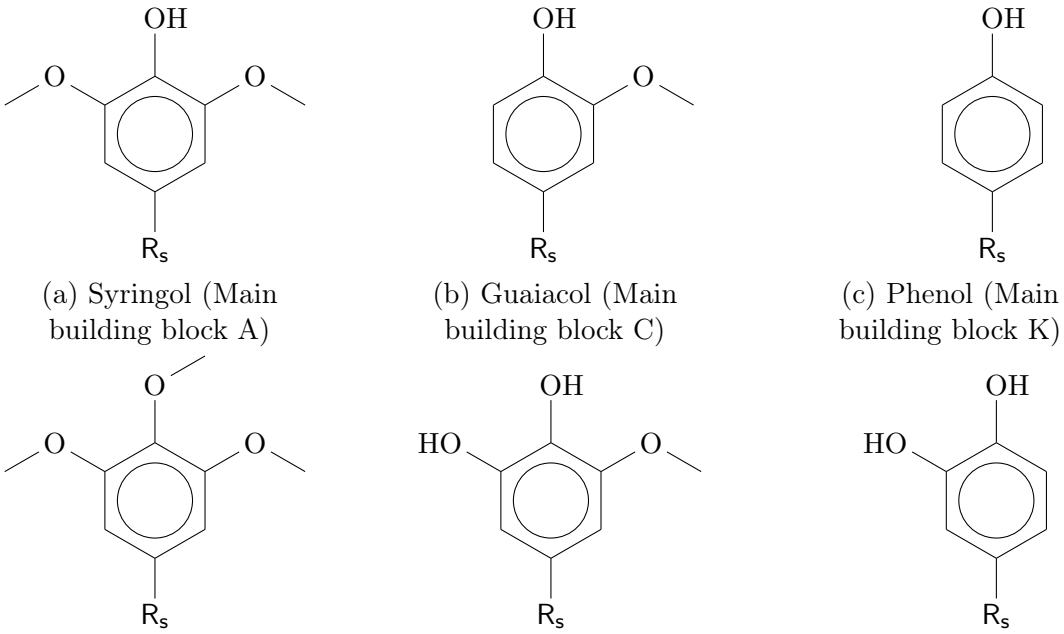

(a) Syringol (Main building block A)
(b) Guaiacol (Main building block C)
(c) Phenol (Main building block K)
(d) Dimethoxyanisole (Main building block Q)
(e) 3-Methoxycatechol (Main building block T)
(f) Catechol (Main building block U)

Figure 1: Main building blocks of lignin pyrolysis oil components. R_s denotes a side chain as introduced in Figs. 3 to 6. Names are given assuming H as side chain.

lead to 276 different compounds which are used forthwith to represent the lignin pyrolysis oil. In this study all combinations of main building blocks and side chains have been taken

into account, although the presence of not all of them has been verified experimentally in literature. The reason for this is threefold: First, within the vast amount of different components they may be present but not detected so far. Second, even if they are not present, (minor) changes in the process conditions could possibly favor their production. Third, this systematic approach may allow the identification of possible trends.

Upgrading

As pyrolysis oil is not suited for direct usage in SI ICEs, upgrading is required[23,24]. HDO is considered to be the most promising way of converting pyrolysis oil into fuels[23,24]. Hydrogen is added to remove oxygen from the molecules, to hydrogenate double bonds and aromatic rings. Applying these HDO reactions[25] to the side chains leads to the reaction pathways shown in Figs. 3 to 6. For the main building blocks, the reactions proceed via the pathways depicted in Fig. 2. Other reactions such as demethylation or decarboxylation are thus not considered herein, as these reactions do not produce new side chains. On the other hand, these reactions lower the carbon efficiency and are therefore not desirable.

For aliphatic rings, dehydration may generate double bonds within the ring or on its substituents. These side chains are only considered in conjunction with aliphatic rings. In the case of aromatic rings, these intermediate steps (e.g. in Fig. 3 shown with a dashed arrow) are skipped. Considering every possible combination of side chain and main building block, 1679 different molecules need to be evaluated as fuel. To facilitate the reference to the respective compounds, the following naming convention is introduced: the main building blocks are identified by a combination of letters whereas the side chains are numbered. The corresponding labels are shown in Figs. 2 to 6, e.g. methylcyclohexane is denoted as N2.

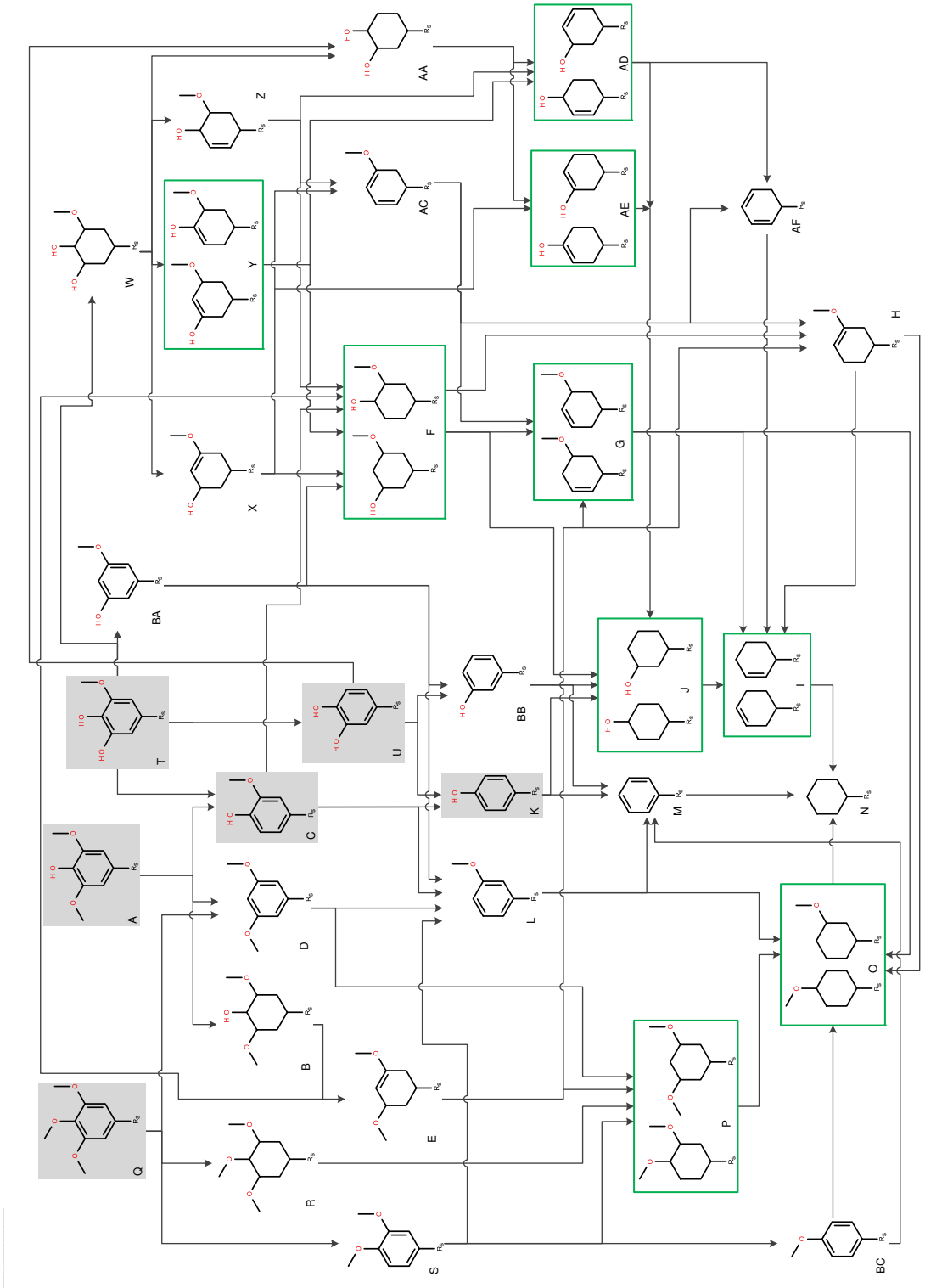

Figure 2: HDO reaction network of the main building blocks. The main building blocks identified in lignin pyrolysis oil[10,21,22] are shaded in gray (see Fig. 1). Fragments framed in green represent compounds whose structures cannot be distinguished by means of Group Contribution Methods. R_s denotes any side chain shown in Figs. 3 to 6.

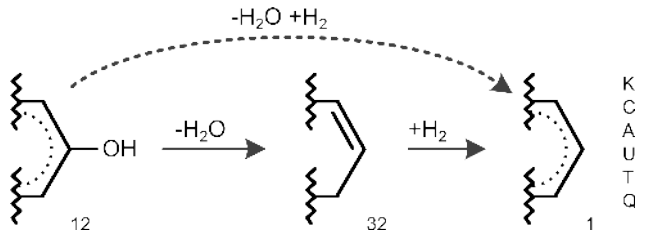

Figure 3: HDO upgrading pathway of a hydroxy group. The dashed arrow indicates the upgrading of phenolic compounds. The numbers represent the ID of the respective side chain. The letters identify the main building blocks in combination with which the respective side chain were reported in the literature.

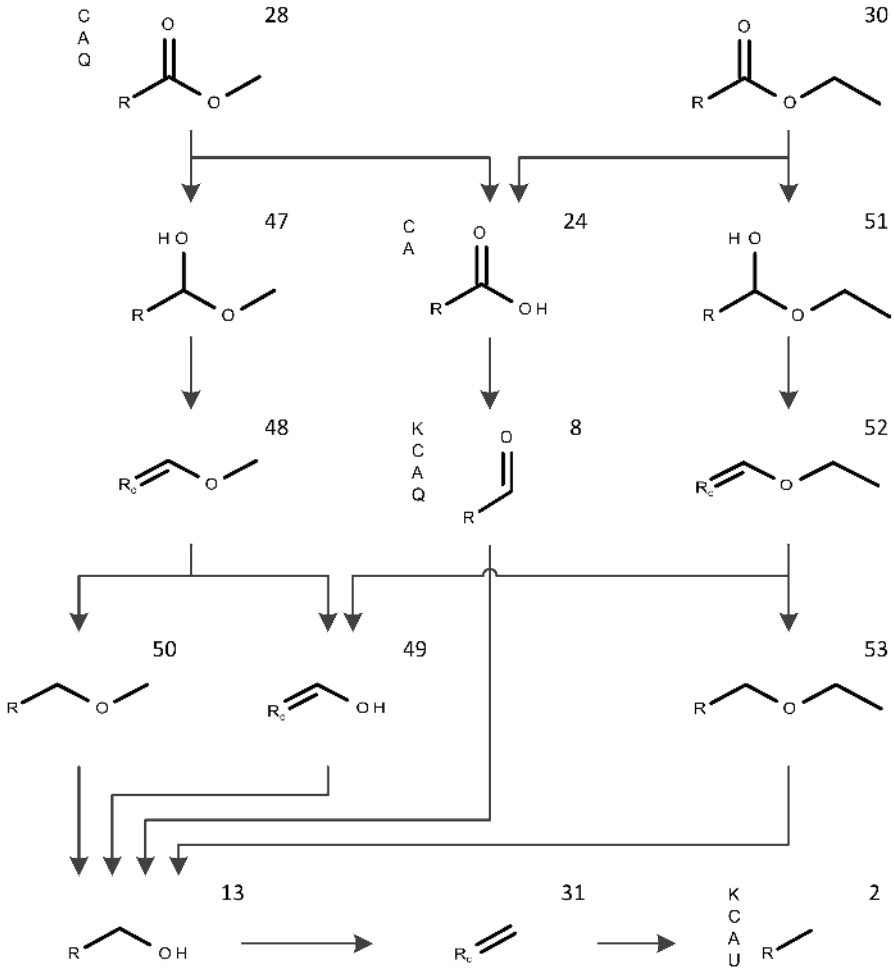

Figure 4: HDO upgrading pathway of different side chains leading to a final chain length of 1 C atoms. R denotes any ring structure according to Fig. 2, while R_c stands for aliphatic rings only. The numbers represent the ID of the respective side chain. The letters identify the main building blocks in combination with which the respective side chain were reported in the literature.

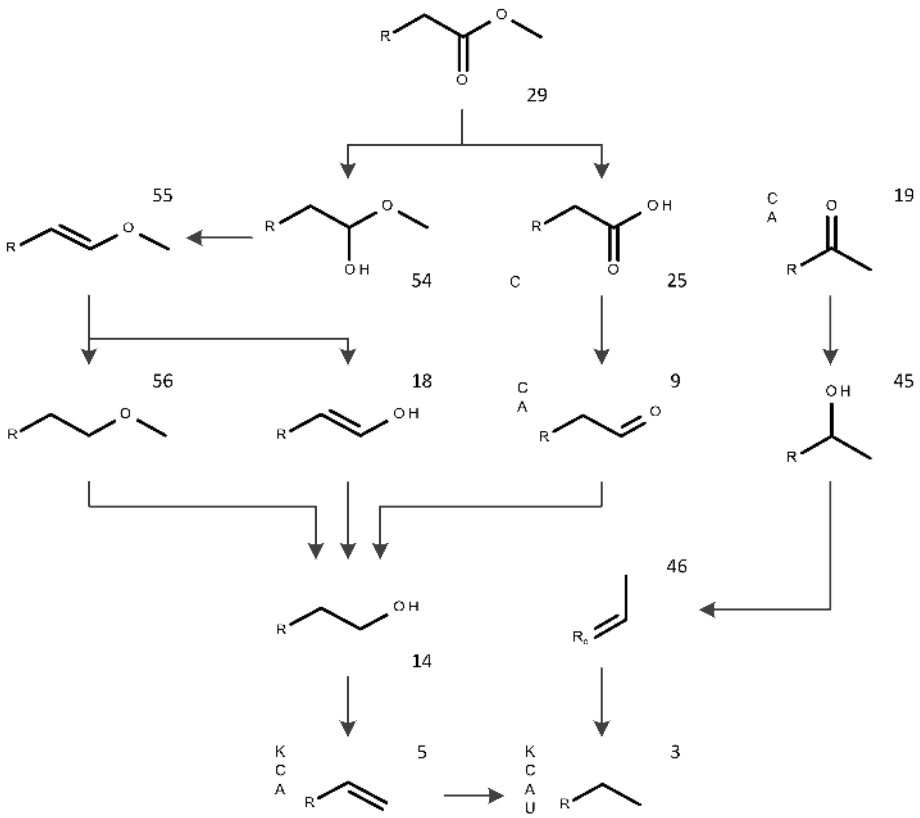

Figure 5: HDO upgrading pathway of different side chains leading to a final chain length of 2 C atoms. R denotes any ring structure according to Fig. 2, while R_c stands for aliphatic rings only. The numbers represent the ID of the respective side chain. The letters identify the main building blocks in combination with which the respective side chain were reported in the literature.

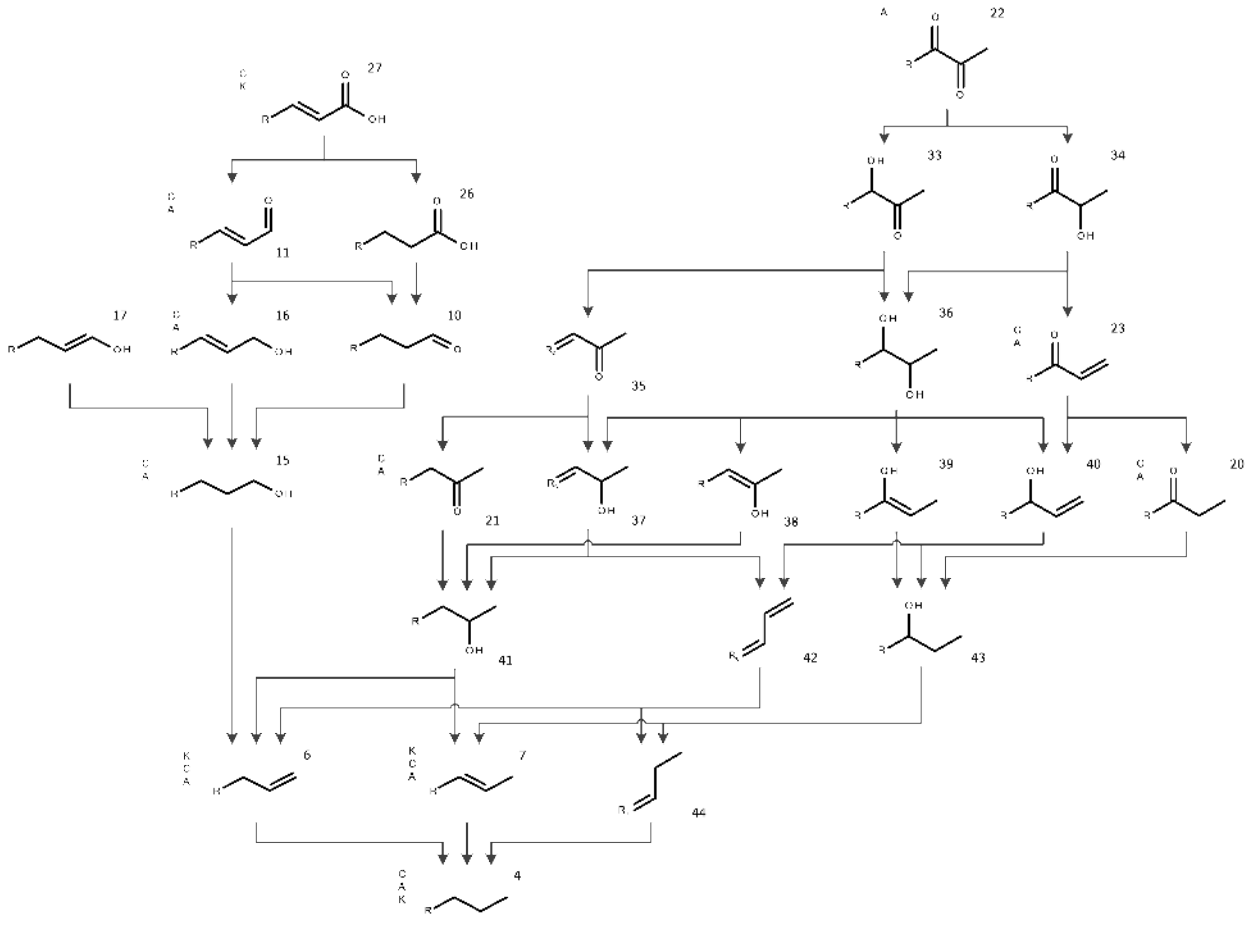

Figure 6: HDO upgrading pathway of different side chains leading to a final chain length of 3 C atoms. R denotes any ring structure according to Fig. 2, while R_c stands for aliphatic rings only. The numbers represent the ID of the respective side chain. The letters identify the main building blocks in combination with which the respective side chain were reported in the literature.

Method

ICE Model

The suitability of a certain compound as replacement for gasoline was judged using an ICE model[26]. The model was built to investigate the influence of fuel properties on the performance of a Direct Injection (DI) SI engine. The engine was optimized automatically for each fuel such that the fuel is used to its full potential. Therefore, efficiency at the brake was optimized at 2000 rpm and at a charging pressure of 2 bar (full load) by adapting the compression ratio (restricted by the occurrence of knocking). While adapting the compression ratio the bore-to-stroke ratio and total cylinder volume were kept constant at 0.97 and 535 cm^3, respectively. Using a simple car model, quasi-stationary simulations allowed to model the performance of a compound over a standard driving cycle.

As input parameters the elemental composition ($C_xH_yO_z$), liquid density (ρ), liquid kinematic viscosity (ν), vapor heat capacity ($c_{p,\mathrm{g}}$), vapor pressure (p_{vap}), enthalpy of vaporization (h_{vap}) and the RON were required. Details of the model have been reported elsewhere[26].

Within this study, the efficiency, the specific CO_2 emissions at 2000 rpm and full load (2 bar charging pressure) as well as the volumetric fuel consumption over the worldwide harmonized light vehicles test cycle (WLTC) were evaluated.

Property Estimation

Due to the lack of experimental data for most of the studied compounds, all properties of interest were estimated using Group Contribution Methods (GCMs): Vapor heat capacity[27], liquid density, boiling and melting point, autoignition temperature, enthalpy of vaporization[28] and liquid viscosity[29]. The liquid density is calculated using the GCM for the liquid molar volume. The vapor pressure is calculated based on the estimated boiling point and the enthalpy of vaporization using the Clausius-Clapeyron equation. In Table 1 an overview of the estimation errors (Average Absolute Error (AAE) and Average Relative Error (ARE)),

as reported by the respective authors, is given. These GCMs were selected according to the

Table 1: Overview on the Average Absolute Error and Average Relative Error of the chosen GCMs.

	AAE	ARE [%]
boiling point (T_{boil}))	5.96 K	1.38
melting point (T_{melt})	15.99 K	5.07
enthalpy of vaporization (h_{vap})	1.29 kJ/mol	3.24
autoignition temperature (T_{auto})	13.51 K	2.09
liquid molar volume (V_{mol})	0.0024 cm^3/kmol	2.03
kinematic viscosity (ν)	n/a	9.2
vapor heat capacity ($c_{p,\mathrm{g}}$)	5.9 J/(mol K)	n/a

recommendation of another study[30], with the exception of the viscosity. For this parameter, a slightly less accurate method with the benefit of the group definitions matching the definitions of the other methods was chosen. Although these GCMs use the structure of the molecule to estimate its properties, they are unable to distinguish certain isomers with aliphatic rings. Within Fig. 2 these isomers are marked with a green frame. As it can be seen, these isomers differ by the position of the substituents in the ring.

As a GCM to predict the RON was not available, another approach was employed. Using experimental data[31–39], the following correlation for the RON based on the autoignition temperature (T_{auto})[40–42], the number of hydrogen atoms (y) and the normal boiling point (T_{boil})[40,43] was developed.

$$\begin{aligned}\mathrm{RON} =& 116.44 - 0.26 \exp\left(\frac{2557.48}{T_{\mathsf{auto}}}\right) + 8.13 \times 10^{-5} y^{4.38} \\ & - 1.73 \times 10^{-6} \exp\left(\frac{2557.48}{T_{\mathsf{auto}}}\right) y^{4.36} - 5.94 \times 10^{14} \frac{y^{4.36}}{T_{\mathsf{boil}}^{7.45}}\end{aligned} \tag{1}$$

with a residual standard error of 11.2, an R^2 of 0.8251 and an F-statistic of 141.5.

Boundary Conditions

As the fuel must be liquid during operation, thresholds regarding the melting point (T_{melt}) and the boiling point (T_{boil}) were specified. Two different ranges were defined based on the climate of Central Europe: For all-year fuels: $T_{\mathsf{melt}} \leq 253\,\mathrm{K}$ and $T_{\mathsf{boil}} \geq 333\,\mathrm{K}$, and for summer fuels: $T_{\mathsf{melt}} \leq 273\,\mathrm{K}$ and $T_{\mathsf{boil}} \geq 333\,\mathrm{K}$. Additionally, an upper limit for the boiling point was specified at 463 K according to T_{90}, the temperature where 90 % of the mixture is evaporated, as defined by ASTM D4814[44]. The estimated properties of all compounds meeting these requirements were used as input parameters for the SI ICE model.

Results & Discussion

Compliance with Boundary Conditions

Fig. 7, shows the boiling and the melting points of all compounds. The red horizontal lines represent the thresholds of the boiling point, while the vertical red solid and dashed lines show the limit of the melting point for all-year and summer fuel, respectively. Among the 1679 compounds, 142 compounds satisfy these boundary conditions – 107 are suitable for use as fuel year-round, while an additional 35 are suited for summer operation only because of their higher melting points.

Group Influences

To discuss the influence of the functional groups on the compliance with the previously defined thresholds, the number of molecules following the criteria is plotted against the number of each specific functional group present in the molecule (Fig. 8). For example when studying the case of the CO group one can see that there is a total of 1492 ($= 1366 + 30 + 96$) compounds without a CO group. Furthermore, there are no groups with more than two CO groups and 33 with two CO groups, all of them are not suited as fuel due to the boundary

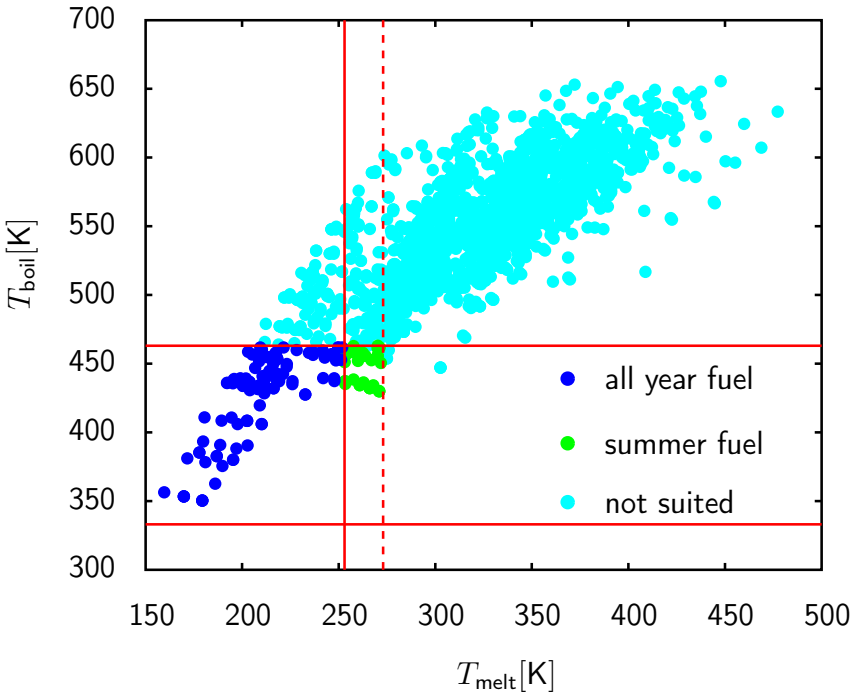

Figure 7: Estimation of melting and boiling points of the studied compounds. Dark blue: compounds suited as all-year fuel, green: fulfilling only summer fuel specifications and light blue: not compliant within any of the ranges. Red lines: temperature thresholds.

conditions. The case with one CO group is more interesting where 5 compounds are suited as summer fuel and 11 fulfill the specification as all year fuel. Finally there are 138 compounds left with one CO group considered not suited as fuel. Based on this analysis it becomes evident that all $-$COOH and $-$COOR groups need to be removed. Furthermore, it can be concluded that no more than one oxygen atom is allowed per molecule. $-$CHO groups are only suited for summer fuels. The influence of double bonds on the melting point and thereby the boundary conditions is less pronounced. In summary, the presence of hydrogen bonds in these molecules has a strong influence on the melting point. It mostly determines whether a compound is still liquid in the temperature range of interest. All compounds have boiling points above 333 K.

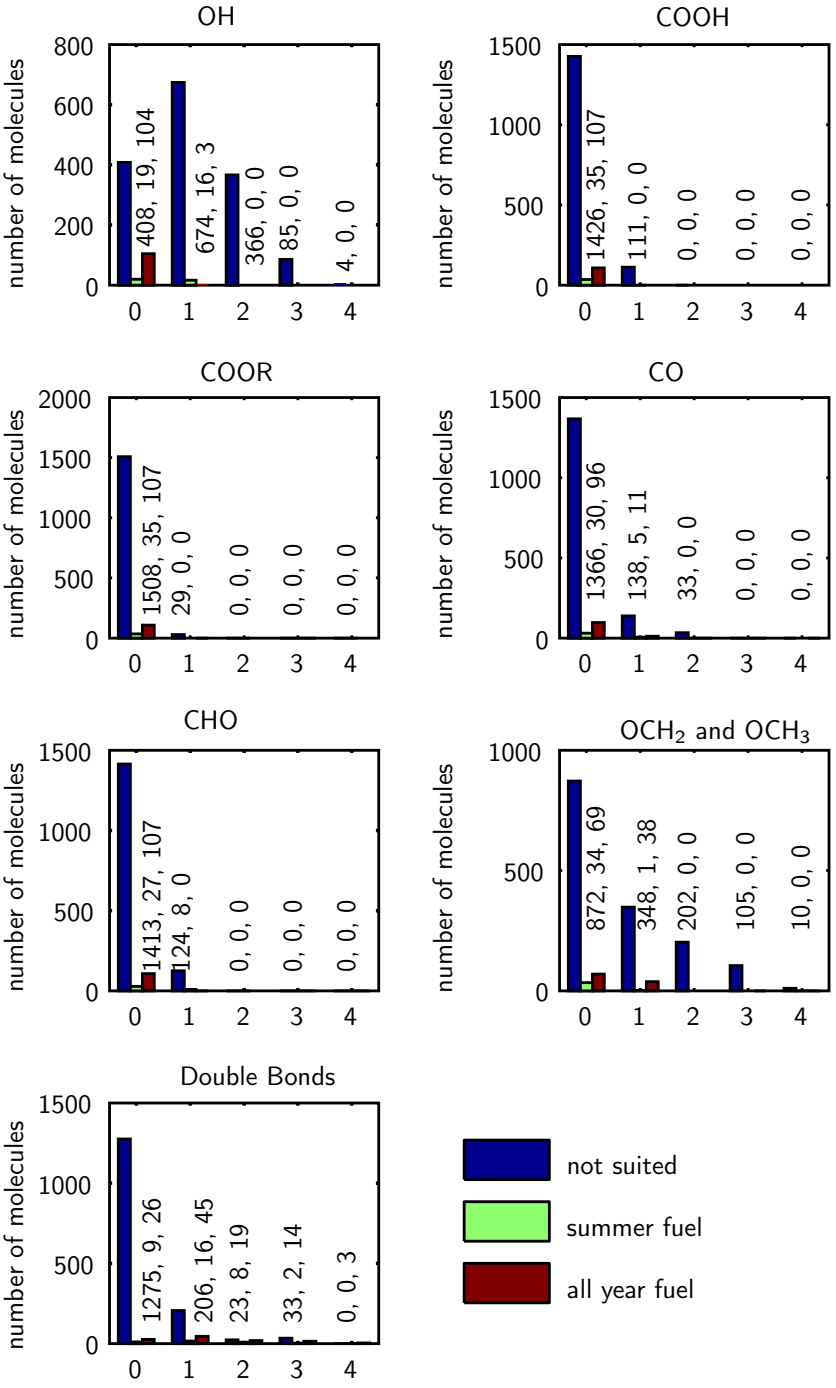

Figure 8: Histograms for the different functional groups categorized according to the three temperature ranges. The y-axis shows the number of molecules satisfying the criteria; the x-axis, the occurrence per molecule. Compounds without the functional group in question are situated at $x = 0$. The numbers show the values for each category in the following order: not suited, summer fuel, all-year fuel.

Optimized Selection

The compounds fulfilling the different criteria (efficiency, specific CO_2 emissions, and volumetric fuel consumption) best are shown in Fig. 9. It is important to note that the suitability of a compound as fuel depends on its performance in the engine. The compounds that are present in all selections consequently represent a compromise of the three criteria and are not necessarily the best overall performers. The suitability of the 142 molecules suitable for all-year or summer operation as pure fuel was subsequently analyzed.

Depending on the optimization criteria the number of compounds was reduced to 24 (28) with efficiency (η), 12 (13) with specific CO_2 emissions and 5 (11) with volumetric fuel consumption (c) as criteria, respectively (values given for all-year fuels, values for summer fuels in parenthesis). The structures in Fig. 9 suggest aromatics to be favorable in terms of volumetric fuel consumption. This can be attributed to their high Lower Heating Value (LHV) as well as their high RON. On the other hand, molecules with a higher degree of saturation are advantageous regarding specific CO_2 emissions as the fraction of carbon atoms present is reduced, leading to lower specific CO_2 emissions. The presence of a >CO group seems to be beneficial for each criterion, in particular efficiency where it is present in the two top performing molecules 1-cyclohexa-2,4-dien-1-ylpropan-1-one (AF20) and 1-cyclohexa-2,4-dien-1-ylpropan-2-one (AF21). $-OCH_3$ and $-OCH_2-$ groups improve the efficiency and lower specific CO_2 emissions and are always attached to non-aromatic rings. Due to the impact of $-OH$ groups on the melting point, compounds containing those are only suitable as summer fuels. Comparing for example cyclohexanol (J1) with cyclohexane (N1), it can be seen that the presence of the $-OH$ group significantly improves the suitability of the compound as SI fuel. The efficiency increases from 31.1 % to 35.2 %. Specific CO_2 emissions and volumetric fuel consumption are reduced from 0.83 g/kWh to 0.77 g/kWh, 8.7 l/100 km to 7.6 l/100 km, respectively.

Table 2 summarizes the performance parameters together with the average amount of H_2 added for each selection. Minimum, average and maximum values are reported. An

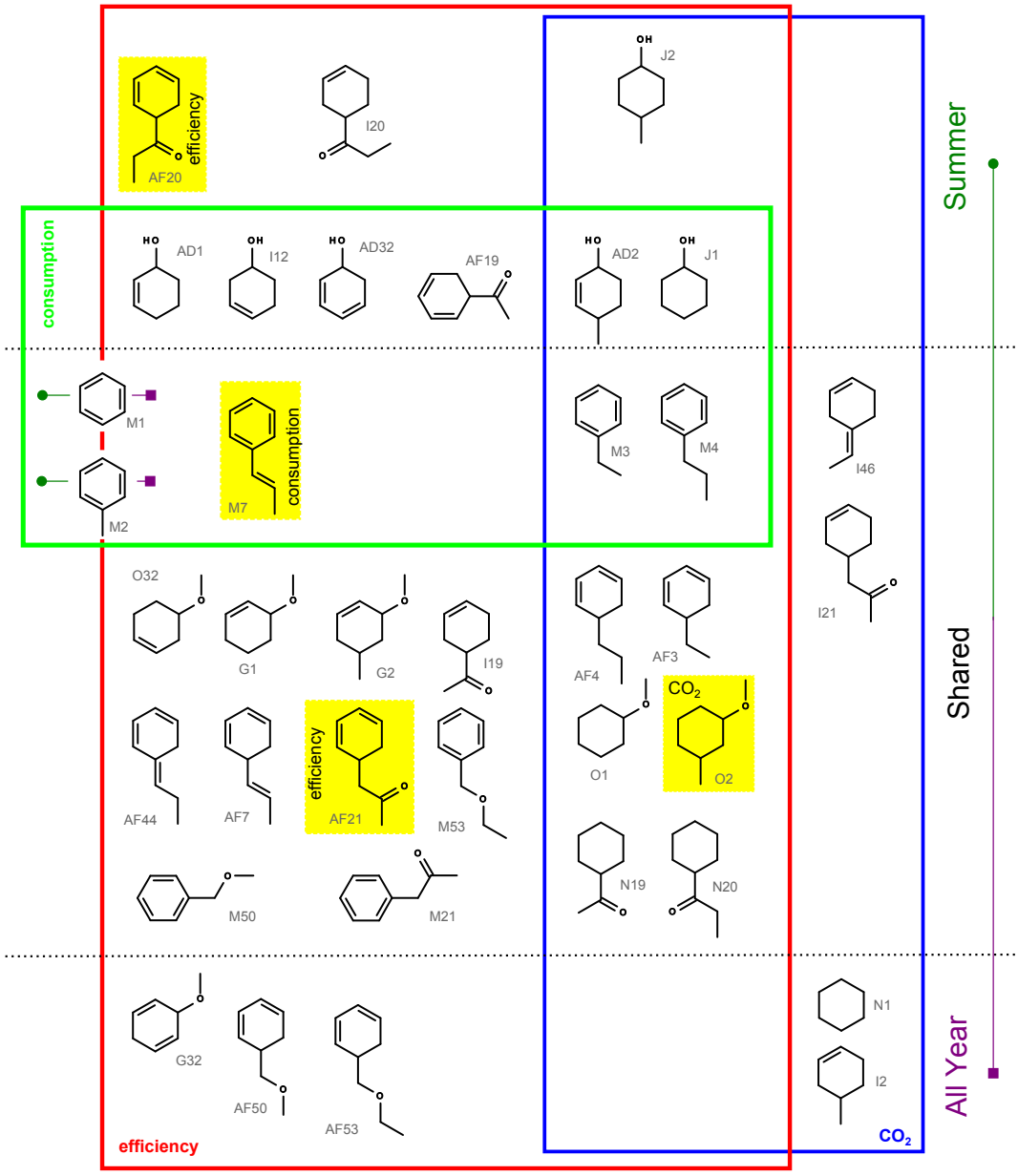

Figure 9: Euler diagram showing the selection of compounds with either optimized efficiency (red), specific CO_2 emissions (blue) or volumetric fuel consumption (green). On top: summer fuels (green dots), in the middle: shared compounds, at the bottom: compounds only present in the all-year fuel selection (violet squares). The best performing molecules are highlighted in yellow together with the parameter they optimize.

overall summary of the results for each compound can be found in Table 4 in the Appendix. Additionally the values for gasoline, *n*-butanol and α-pinene are listed as reference[26]. As a reference, full HDO of the lignin pyrolysis oil to cyclohexane derivatives requires on average 7.05 $\mathrm{mol_{H_2}/mol_{oil}}$ (minimum 4, maximum 10 $\mathrm{mol_{H_2}/mol_{oil}}$). In terms of H_2 addition, roughly 55 % to 70 % of the maximum is needed, with all-year fuels requiring less H_2 addition than summer fuels. The amount of H_2 added for optimized selections increases in the following order: volumetric fuel consumption < efficiency < specific CO_2 emissions. Minimum efficiency is, with one exception, higher than for gasoline. Average efficiency is in the order of *n*-butanol for the all-year fuel selections. Minimum CO_2 emissions are similar to gasoline. An optimization for volumetric fuel consumption shows values below α-pinene with maximum values comparable to gasoline.

Single Compounds

Concerning single compounds, the best performing molecules as indicated in Fig. 9 are listed together with their performance values in Table 3. In any case, minimum volumetric fuel consumption is achieved with β-methylstyrene (M7). Efficiency is optimized in the summer selection with 1-cyclohexa-2,4-dien-1-ylpropan-1-one (AF20). In the all-year selection, efficiency is maximized with 1-cyclohexa-2,4-dien-1-ylpropan-2-one (AF21). Specific CO_2 emissions are minimized with 1-methoxy-4-methylcyclohexane (O2).

Based on its respective properties 4-methylanisole (BC2) has been identified as best suited drop-in fuel obtainable from pyrolysis oil[45]. Anisole (BC1) has been included in a list of 40 bioblendstocks with desirable properties[46]. The simulation results shown in Table 3 indicate that both 4-methylanisole and anisole perform, with the exception of CO_2 emissions, well. However none of these two molecules performs best with respect to either efficiency, specific CO_2 emissions or volumetric fuel consumption.

Table 2: Summary of the performance parameters (efficiency (η), specific CO_2 emissions ($e_{CO_2,FL}$) both at full load, and volumetric fuel consumption (c), specific CO_2 emissions ($e_{CO_2,D}$) based on the WLTC), including the average H_2 required for production of the different selections of compounds starting from lignin pyrolysis oil. std: standard deviation.

criteria		η [%]	$e_{CO_2,FL}$ [g/kWh]	c [l/100km]	$e_{CO_2,D}$ [g/km]	$\frac{\text{mol } H_2}{\text{mol oil}}$ [–]
all-year						
η	min	34.3	0.76	6.9	191	1.00
	mean	36.2	0.80	7.5	203	4.14
	max	36.9	0.90	8.8	232	8.00
	std	0.5	0.03	0.5	8	1.45
CO_2	min	31.1	0.76	7.1	191	1.00
	mean	35.8	0.78	7.5	198	4.88
	max	36.4	0.83	8.8	207	8.00
	std	0.8	0.02	0.6	5	1.39
c	min	34.3	0.79	6.9	202	1.00
	mean	35.7	0.83	7.2	211	3.90
	max	36.2	0.90	7.9	232	7.00
	std	0.7	0.03	0.3	9	1.26
summer fuel						
η	min	34.9	0.76	6.9	191	1.00
	mean	36.3	0.79	7.3	201	4.19
	max	37.1	0.85	8.8	216	8.00
	std	0.4	0.03	0.4	7	1.41
CO_2	min	34.3	0.76	7.1	191	1.00
	mean	36.0	0.78	7.5	197	4.83
	max	36.8	0.80	8.8	204	8.00
	std	0.4	0.02	0.6	5	1.38
c	min	34.3	0.77	6.9	196	1.00
	mean	35.9	0.82	7.2	207	4.01
	max	36.8	0.90	7.9	232	7.00
	std	0.6	0.03	0.2	8	1.29
reference[26]						
gasoline		33.7	0.77	8.2	193	
n-butanol		36.5	0.70	9.3	179	
α-pinene		32.8	0.84	7.6	211	

Table 3: Performance of the molecules when optimizing engine performance. Lowest volumetric fuel consumption: β-methylstyrene (M7). Maximum efficiency in summer fuel selection: 1-cyclohexa-2,4-dien-1-ylpropan-1-one (AF20). Maximum efficiency in all-year fuel selection: 1-cyclohexa-2,4-dien-1-ylpropan-2-one (AF21), minimum specific CO_2 emissions: 1-methoxy-4-methylcyclohexane (O2). Bioblendstock: anisole (BC1)[46], Optimum drop-in fuel: 4-methylanisole (BC2)[45].

molecule	η_{FL} [%]	η_{PL} [%]	P_{FL} [kW]	$e_{\mathrm{CO_2,FL}}$ [kg/kWh]	$\varepsilon_{\mathrm{CR}}$ [–]	η_{cyc} [%]	$e_{\mathrm{CO_2,D}}$ [g/km]	c [l/100km]
AF20	37.1	22.4	81.4	0.81	12.7	22.9	205	7.0
AF21	36.9	22.2	80.9	0.81	12.2	22.8	206	7.4
M7	36.2	21.8	78.7	0.83	11.8	22.4	211	6.9
O2	35.5	21.6	77.3	0.76	9.4	22.0	191	8.6
BC1	36.3	21.8	80.7	0.89	14.8	22.5	227	7.8
BC2	36.8	22.2	81.2	0.85	13.8	22.8	216	7.5

Influence of Selected Groups

Based on these findings, the influence of the different groups on the performance as fuel is investigated. Cyclohexane (N1) is chosen as base molecule, to which the selected groups ($-CH_3$, $-CHO$, $-COCH_3$, $-COOCH_3$, $-OCH_3$, $-OH$) are subsequently attached. At first the influence on the different input properties (x_i) is calculated:

$$\Delta x_i = x_i - x_{i,\mathsf{N1}} \tag{2}$$

Based on these deviations, the averaged absolute difference ($\overline{\Delta x_i}$) is used to determine the local sensitivities around cyclohexane. By combining the local derivative with the difference in the input property it is possible to estimate its influence on efficiency ($\delta\eta_i$).

$$\delta\eta_i = \frac{\eta(x_{i,\mathsf{N1}} + 0.5\overline{\Delta x_i}) - \eta(x_{i,\mathsf{N1}} - 0.5\overline{\Delta x_i})}{\Delta x_i} \left(x_i - x_{i,\mathsf{N1}}\right) \tag{3}$$

$\delta\eta_i$ can be interpreted as the local derivative of the efficiency. Although it is difficult to translate this directly to a defined change in efficiency, this formulation allows detecting amplification/reduction and inverse correlations quickly.

Fig. 10 presents the results of this investigation. The changes in viscosity, vapor pressure and enthalpy of vaporization for cyclohexanol are most prominent, whereas the influence of the viscosity on the efficiency is non existent. This behavior can be explained by the fact that the viscosity influences droplet size. However, as long as the droplets evaporate in a given time, there is no influence on the efficiency. Additionally the power requirement of the fuel pump is negligible[26], changes in its power requirement due to increase viscosity are thus not expected to be significant. The opposite is true for changes in heat capacity, autoignition temperature/RON and density, where even small changes are amplified. Changes in vapor heat capacity lead to changes in temperature at Top Dead Center (TDC) and thus influence the thermodynamic cycle. The influence of the RON can be explained by the fact that the maximum compression ratio is knock-limited. The influence of the enthalpy of vaporization is due to the fact that an increase in enthalpy of vaporization leads to lower temperatures, which is favorable in terms of knock reduction. However according to Carnot, lower temperatures also lead to lower efficiencies. Furthermore, a higher enthalpy of vaporization increases charge cooling, which in turn allows for more fuel–air mixture to be introduced into the cylinder. Which of these mechanisms prevails depends on the detailed situation. As long as the optimum compression ratio cannot be reached due to knock limitation, it is to be expected that any efficiency loss due to lower temperatures will be outweighted by efficiencies gains due to increased compression ratios. Once the optimum compression ratio is obtained, the situation looks different. The influence of the enthalpy of vaporization warrants further investigations. Increasing the size of the molecule leads to negative influences in case of additional carbon (x) and hydrogen (y) atoms and positive effects for additional oxygen atoms (z). The elemental composition defines the LHV and the mixture composition of the burnt gases. Thereby the elemental composition has a direct influence on the thermodynamic

cycle. The impact of the vapor pressure on efficiency is relatively small and inverse. This can be explained by the fact that as long as the fuel is fully evaporated within the given time there is no impact of the vapor pressure on efficiency.

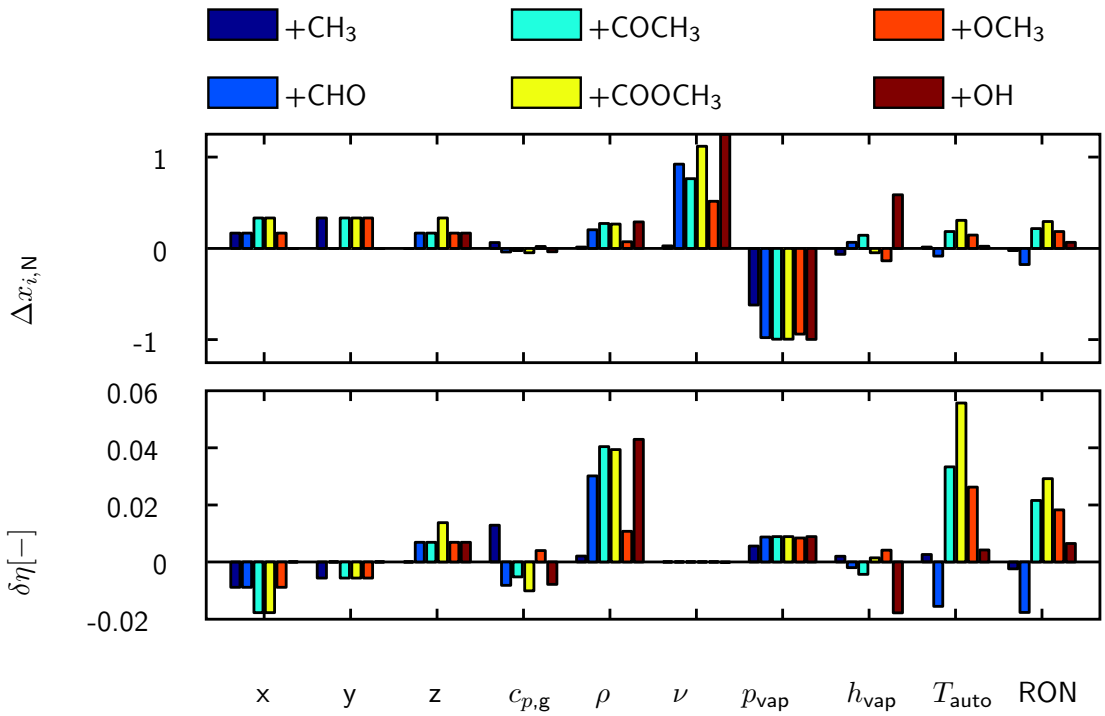

Figure 10: Fuel properties and efficiency dependency on functional groups attached to cyclohexane. The change in property is normalized with respect to the values of cyclohexane, except for the number of oxygen atoms (z) that is normalized using the number of carbon atoms in cyclohexane. The change in viscosity for cyclohexanol is equal to 9.02.

Conclusion

The most suitable compounds in lignin-derived pyrolysis oil to replace gasoline were identified, by coupling an engine model with a reaction pathways network,. Fuels showing higher efficiencies than the currently-employed fuels can be produced from pyrolysis oil by selective hydrotreating. It is impossible to lower the specific CO_2 emissions compared to n-butanol substantially. However, compared to gasoline this equals a reduction by roughly 10 %. On the contrary, specific CO_2 emissions in the range of gasoline are expected. Yet, the volumetric fuel consumption can be significantly reduced if this is the aim of the optimization.

The influence of selected groups ($-CH_3$, $-CHO$, $-COCH_3$, $-COOCH_3$, $-OCH_3$, $-OH$) as cyclohexane side chains on the fuel properties and efficiency was shown.

Based on these results, we derived the following design rules:

- Full HDO is not beneficial for the fuel quality. In addition, partial HDO requires less H_2 and thereby reduces process costs significantly.
- To comply with the defined limitations on both melting and boiling point, only one oxygen atom is allowed per molecule.
- $-COOH$ and $-COOR$ groups must be completely removed to meet the required melting and boiling point ranges (besides issues with corrosion in case of $-COOH$ groups).
- Compounds with a CHO group are only suitable as summer fuels.
- Structural entities with one $>CO$, a $-OCH_2-$ or with a $-OCH_3$ group attached to non-aromatic rings contribute to good overall performance. While $-OCH_2-$ and $-OCH_3$ groups improve almost all properties (except carbon and hydrogen content), $>CO$ groups lead to improvements in density and RON but worsening in heat capacity and carbon content, when compared to $-OCH_3$.

Acknowledgement

We would like to thank P. Soltic (Empa) and D. Wüthrich for sharing their knowledge on engines and the countless hours of discussions about the model, L. Bärtsch for the support with programming, and D. Scholz for his support with chemical questions.

Supporting Information Available

Appendix

Table 4: Results for all compounds shown in Fig. 9. Efficiency (η) and specific CO_2 emissions (CO_2) at full load, consumption (c) and specific CO_2 emissions (CO_{2cyc}) over the WLTC. SU: summer fuel, AY: all year fuel.

	η [%]	CO_2 [g/kWh]	c [l/100 km]	CO_{2cyc} [g/km]	condition & criteria	IUPAC name
AD1	36.5	0.79	7.3	200	SU: η, c	2-cyclohexenol
AD2	36.8	0.77	7.2	196	SU: η, c, CO_2	4-methyl-2-cyclohexen-1-ol
AD32	36.6	0.83	7.2	211	SU: η, c	cyclohexa-2,4-dien-1-ol
AF19	36.7	0.83	7.1	211	SU: η, c	1-cyclohexa-2,4-dien-1-ylethanone
AF20	37.1	0.81	7.0	205	SU: η	1-cyclohexa-2,4-dien-1-ylpropan-1-one
AF21	36.9	0.81	7.4	206	SU & AY: η	1-cyclohexa-2,4-dien-1-ylpropan-2-one
AF3	36.4	0.77	7.2	195	AY & SU: η, CO_2	5-ethyl-1,3-cyclohexadiene
AF4	36.4	0.76	7.2	193	AY & SU: η, CO_2	5-propylcyclohexa-1,3-diene
AF44	36.4	0.77	7.2	195	AY & SU: η	(5Z)-5-propylidenecyclohexa-1,3-diene
AF50	36.4	0.80	7.8	204	AY: η	5-(methoxymethyl)-1,3-cyclohexadiene
AF53	35.6	0.81	7.9	205	AY: η	5-(ethoxymethyl)cyclohexa-1,3-diene
AF7	36.4	0.80	7.7	202	AY & SU: η	5-[(1E)-1-Propen-1-yl]-1,3-cyclohexadiene

Table 4 - *continued*

	η [%]	CO_2 [g/kWh]	c [l/100 km]	CO_{2cyc} [g/km]	condition & criteria	IUPAC name
G1	36.2	0.78	8.7	198	AY & SU: η	4-methoxycyclohexene
G2	36.5	0.77	8.4	195	AY & SU: η	5-methoxy-3-methyl-cyclohexene
G32	36.5	0.82	8.5	204	AY: η	dihydroanisole
I12	36.5	0.79	7.3	200	SU: η, c	3-cyclohexen-1-ol
I19	36.5	0.80	7.2	203	AY & SU: η	4-acetylcyclohexene
I2	34.1	0.80	8.1	206	AY: CO_2	4-methylcyclohexene
I20	36.7	0.78	7.1	199	SU: η	1-cyclohex-3-en-1-ylpropan-1-one
I21	36.4	0.79	7.6	201	AY & SU: CO_2	1-(3-Cyclohexen-1-yl)acetone
I46	34.3	0.79	7.7	199	AY & SU: CO_2	4-ethylidenecyclohexene
J1	35.2	0.77	7.6	196	SU: η, c, CO_2	cyclohexanol
J2	34.9	0.77	7.6	196	SU: η, CO_2	4-methylcyclohexanol
M1	34.3	0.90	7.9	232	SU: c AY: η, c	benzene
M2	34.5	0.87	7.6	221	SU: c AY: η, c	toluene
M21	36.7	0.85	7.3	216	AY & SU: η	phenylacetone
M3	36.1	0.80	7.1	204	AY & SU: η, c, CO_2	ethylbenzene
M4	36.0	0.79	7.1	202	AY & SU: η, c, CO_2	n-propylbenzene
M50	36.2	0.84	7.7	214	AY & SU: η	(methoxymethyl)benzene
M53	35.4	0.85	7.9	215	AY & SU: η	(ethoxymethyl)benzene
M7	36.2	0.83	6.9	211	AY & SU: η, c	β-methylstyrene

Table 4 - *continued*

	η [%]	CO_2 [g/kWh]	c [l/100 km]	CO_{2cyc} [g/km]	condition & criteria	IUPAC name
N1	31.1	0.83	8.7	207	AY: CO_2	cyclohexane
N19	36.2	0.77	7.3	196	AY & SU: η, CO_2	methyl cyclohexyl ketone
N20	36.3	0.76	7.2	194	AY & SU: η, CO_2	ethyl cyclohexyl ketone
O1	35.4	0.76	8.8	193	AY & SU: η, CO_2	methoxycyclohexane
O2	35.5	0.76	8.6	191	AY & SU: η, CO_2	1-methoxy-4-methylcyclohexane
O32	36.2	0.78	8.7	198	AY & SU: η	4-methoxycyclohexene

References

(1) Zakzeski, J.; Bruijnincx, P. C. A.; Jongerius, A. L.; Weckhuysen, B. M. *Chemical Reviews* **2010**, *110*, 3552–3599.

(2) Elliott, D. C. *Energy & Fuels* **2007**, *21*, 1792–1815.

(3) No, S.-Y. *Renewable and Sustainable Energy Reviews* **2014**, *40*, 1108–1125.

(4) Barth, T.; Kleinert, M. *Chemical Engineering & Technology* **2008**, *31*, 773–781.

(5) Linck, M.; Felix, L.; Marker, T.; Roberts, M. *Wiley Interdisciplinary Reviews: Energy and Environment* **2014**, *3*, 575–581.

(6) Lu, Q.; Li, W.-Z.; Zhu, X.-F. *Energy Conversion and Management* **2009**, *50*, 1376–1383.

(7) Oasmaa, A.; Czernik, S. *Energy & Fuels* **1999**, *13*, 914–921.

(8) Bridgwater, A. *Biomass and Bioenergy* **2012**, *38*, 68–94.

(9) Bulushev, D. A.; Ross, J. R. *Catalysis Today* **2011**, *171*, 1–13.

(10) Mu, W.; Ben, H.; Ragauskas, A.; Deng, Y. *Bioenergy Research* **2013**, *6*, 1183–1204.

(11) Saidi, M.; Samimi, F.; Karimipourfard, D.; Nimmanwudipong, T.; Gates, B. C.; Rahimpour, M. R. *Energy Environ. Sci.* **2014**, *7*, 103–129.

(12) Fermoso, J.; Pizarro, P.; Coronado, J. M.; Serrano, D. P. *Wiley Interdisciplinary Reviews: Energy and Environment* **2017**, *6*, e245.

(13) Elliott, D. C.; Hart, T. R.; Neuenschwander, G. G.; Rotness, L. J.; Olarte, M. V.; Zacher, A. H.; Solantausta, Y. *Energy & Fuels* **2012**, *26*, 3891–3896.

(14) Bridgwater, A. *Renewable and Sustainable Energy Reviews* **2000**, *4*, 1–73.

(15) Balat, M.; Balat, M.; Kırtay, E.; Balat, H. *Energy Conversion and Management* **2009**, *50*, 3147–3157.

(16) Oasmaa, A.; van de Beld, B.; Saari, P.; Elliott, D. C.; Solantausta, Y. *Energy & Fuels* **2015**, *29*, 2471–2484.

(17) Heywood, J. B. *Internal Combustion Engine Fundamentals*; McGraw-Hill Education Ltd, 1989.

(18) Boot, M. *Biofuels from Lignocellulosic Biomass: Innovations beyond Bioethanol*; Wiley-VCH Verlag GmbH & Co. KGaA, 2016.

(19) Van de Beld, B.; Holle, E.; Florijn, J. *Applied Energy* **2013**, *102*, 190–197.

(20) Pelaez-Samaniego, M.; Mesa-Pérez, J.; Cortez, L.; Rocha, J.; Sanchez, C.; Marín, H. *Energy for Sustainable Development* **2011**, *15*, 376–381.

(21) Saiz-Jimenez, C.; De Leeuw, J. W. *Organic Geochemistry* **1986**, *10*, 869–876.

(22) Nowakowski, D. J.; Bridgwater, A. V.; Elliott, D. C.; Meier, D.; de Wild, P. *Journal of Analytical and Applied Pyrolysis* **2010**, *88*, 53–72.

(23) Huber, G. W.; Iborra, S.; Corma, A. *Chemical Reviews* **2006**, *106*, 4044–4098, PMID: 16967928.

(24) Mortensen, P. M.; Grunwaldt, J.-D.; Jensen, P. A.; Knudsen, K. G.; Jensen, A. D. *Applied Catalysis A: General* **2011**, *407*, 1–19.

(25) Wang, H.; Male, J.; Wang, Y. *ACS Catalysis* **2013**, *3*, 1047–1070.

(26) Gschwend, D.; Soltic, P.; Edinger, P.; Wokaun, A.; Vogel, F. *Sustainable Energy Fuels* **2017**, *1*, 1991–2005.

(27) Joback, K. G.; Reid, R. C. *Chemical Engineering Communications* **1987**, *57*, 233–243.

(28) Hukkerikar, A. S.; Sarup, B.; Ten Kate, A.; Abildskov, J.; Sin, G.; Gani, R. *Fluid Phase Equilibria* **2012**, *321*, 25–43.

(29) Sastri, S. R. S.; Rao, K. K. *The Chemical Engineering Journal* **1992**, *50*, 9–25.

(30) Nieto-Draghi, C.; Fayet, G.; Creton, B.; Rozanska, X.; Rotureau, P.; de Hemptinne, J.-C.; Ungerer, P.; Rousseau, B.; Adamo, C. *Chemical Reviews* **2015**, *115*, 13093–13164.

(31) American Petroluem Institute, *Technical Data Book - Petroleum Refining*, 6th ed.; 1997.

(32) Al-Fahemi, J. H.; Albis, N. A.; Gad, E. A. M. *Journal of Theoretical Chemistry* **2014**, *2014*, 1–6.

(33) Blurock, E. S. *Computers & Chemistry* **1995**, *19*, 91–99.

(34) Gargiulo, V.; Alfè, M.; Blasio, G. D.; Beatrice, C. *Fuel* **2015**, *150*, 154–161.

(35) Ihara, T.; Tanaka, T.; Wakai, K. *Combustion, Explosion, and Shock Waves* **2009**, *45*, 428–434.

(36) Han, W.-Q.; Yao, C.-D. *Fuel* **2015**, *150*, 29–40.

(37) Yanowitz, J.; Christensen, E.; McCormick, R. L. Utilization of Renewable Oxygenates as Gasoline Blending Components. 2011.

(38) Ryzhov, A. N.; Strizhakova, Y. A.; Smolenskii, E. A.; Lapidus, A. L. *Petroleum Chemistry* **2011**, *51*, 354–362.

(39) Smolenskii, E. A.; Ryzhov, A. N.; Milina, M. I.; Lapidus, A. L. *Doklady Chemistry* **2011**, *436*, 5–10.

(40) Design Institute for Physical Properties, *DIPPR Project 801 - Full Version*; Design Institute for Physical Property Research/AIChE, 2005; 2008; 2009; 2010; 2011; 2012; 2015.

(41) Mitchell, B. E.; Jurs, P. C. *Journal of Chemical Information and Computer Sciences* **1997**, *37*, 538–547.

(42) Lazzús, J. A. *International Journal of Thermophysics* **2011**, *32*, 957–973.

(43) Linstrom, P. J.; Mallard, W. G. *NIST Chemistry WebBook, NIST Standard Reference Database Number 69*; National Institute of Standards and Technology: Gaithersburg MD, 20899, 2005; (retrieved July 21, 2016).

(44) ASTM, *Standard Specification for Automotive Spark-Ignition Engine Fuel*; 2018.

(45) McCormick, R. L.; Ratcliff, M. A.; Christensen, E.; Fouts, L.; Luecke, J.; Chupka, G. M.; Yanowitz, J.; Tian, M.; Boot, M. *Energy & Fuels* **2015**, *29*, 2453–2461.

(46) McCormick, R. L.; Fioroni, G.; Fouts, L.; Christensen, E.; Yanowitz, J.; Polikarpov, E.; Albrecht, K.; Gaspar, D. J.; Gladden, J.; George, A. *SAE International Journal of Fuels and Lubricants* **2017**, *10*.

Graphical TOC Entry